Biophysical Journal
Article

Biophysical Society

# Aligned peptoid-based macrodiscs for structural studies of membrane proteins by oriented-sample NMR

Azamat R. Galiakhmetov,[1] Carolynn M. Davern,[1] Richard J. A. Esteves,[1] Emmanuel O. Awosanya,[1] Quibria A. E. Guthrie,[1] Caroline Proulx,[1] and Alexander A. Nevzorov[1,*]
[1]Department of Chemistry, North Carolina State University, Raleigh, North Carolina

ABSTRACT Development of a robust, uniform, and magnetically orientable lipid mimetic will undoubtedly advance solid-state NMR of macroscopically aligned membrane proteins. Here, we report on a novel lipid membrane mimetic based on peptoid belts. The peptoids, composed of 15 residues, were synthesized by alternating N-(2-phenethyl)glycine with N-(2-carboxyethyl)glycine residues at a 2:1 molar ratio. The chemically synthesized peptoids possess a much lower degree of polydispersity versus styrene-maleic acid polymers, thus yielding uniform discs. Moreover, the peptoid oligomers are more flexible and do not require a specific folding, unlike lipoproteins, in order to wrap around the hydrophobic membrane core. The NMR spectra measured for the membrane-bound form of Pf1 coat protein incorporated in this new lipid mimetics demonstrate a higher order parameter and uniform linewidths compared with the conventional bicelles and peptide-based macrodiscs. Importantly, unlike bicelles, the peptoid-based macrodiscs are detergent free.

SIGNIFICANCE Creating a lipid-rich, highly alignable membrane environment closely mimicking physiological conditions is important for structure-function studies of membrane proteins by solid-state NMR of macroscopically aligned samples. A self-assembled, magnetically oriented, and detergent-free lipid mimetic based on peptoid belts has been developed for the first time. This mimetic yields higher or comparable degree of ordering compared with the commonly used anisotropic bicelles and macrodiscs stabilized by amphipathic peptide and polymer belts. Moreover, conformational flexibility of the synthesized peptoids allows for a higher protein loading compared with lipoprotein-based macrodiscs.

## INTRODUCTION

Oriented-sample (OS) solid-state NMR represents a powerful tool for the structural studies of membrane proteins (MPs). The method generally requires the preparation of a lipid-rich, fully hydrated membrane environment in order to correctly preserve MP folding and functionality. Magnetically aligned bicelles (1–8) have been widely utilized for the structure-function studies of MPs by OS NMR. The native alignment state of bicelles relative to the external NMR field is perpendicular, which arises from the negative susceptibility anisotropy of the hydrophobic alkyl chains (9). The anisotropic bicelles are typically prepared by the mixing of long-chain lipids (mainly DMPC) with short-chain lipids (mainly DHPC) at the molar ratio [DMPC]/[DHPC] >3. Despite their utility for protein structure determination in flat, lipid-rich bilayers, the short-chain DHPC lipids possess detergent-like properties, which may interfere with the structure of the embedded MPs. Therefore, alternative magnetically alignable lipid mimetics have been recently explored including peptide-belt stabilized macrodiscs (10) and macrodiscs encircled by styrene-maleic acid (SMA) copolymer chains (11–13). The former are derived from naturally occurring lipoproteins whose folding largely dictates the overall disc diameter to be around 30 nm, which may make the lipodiscs less stable when loaded with higher amounts of the MP of interest. On the other hand, the high polydispersity of the SMA polymers may result in non-uniformity of the macrodiscs and their order parameters, thus yielding broader NMR lines. Therefore, it would be advantageous to utilize belts that would possess sufficient flexibility to wrap themselves around the DMPC lipid core while having a sufficiently high uniformity in length that, in turn, would make the discs more homogeneous.

Submitted February 17, 2022, and accepted for publication July 17, 2022.
*Correspondence: alex_nevzorov@ncsu.edu
Editor: Charles Deber.
https://doi.org/10.1016/j.bpj.2022.07.024

Synthetic peptoids (14) represent a unique class of highly flexible peptidomimetics that are dominated by side chain chemistry while maintaining the backbone atomic composition of peptides. In short, peptoids are formed by oligomers of N-substituted glycines that have side chains appended to the nitrogen atoms rather than the alpha carbons. Therefore, there is a loss of main-chain chirality and removal of the backbone hydrogen-bond donor (the NH group) (15,16). Peptoids can be easily synthesized to have diverse yet highly controlled amphipathic structures by using solid-phase sub-monomer synthesis (14,16). Due to their similarities to polypeptides and the resistance to proteolytic degradation, peptoid polymers exhibit high biocompatibility. Their effectiveness for biological activities has motivated development for several applications, including vectors for gene and drug delivery (17) and antimicrobial peptidomimetics (18,19). NMR and x-ray studies have demonstrated that peptoid oligomers form secondary helical conformations with the inclusion of alpha-chiral and aromatic side chains (20–24). The partial helical ordering investigated by molecular modeling and circular dichroism has been proposed to be induced by steric clash avoidance and electrostatic repulsion between backbone carbonyls and pi-clouds of side chains with aromatic rings (23,25,26). An important consideration for making peptoid-based macrodiscs is the peptoid-lipid interaction. Similarly to SMA copolymers and lipoprotein peptides, amphipathic peptoids can be inserted into the lipid membrane, leading to the formation of peptoid-lipid fragments (27,28). This interaction with the lipid membrane is driven by the peptoid hydrophobicity on one side and is dependent on the length of the amphipathic peptoid polymer (29–31). In a recent work (32), peptoids were incorporated at the edge of bicelles, and it was demonstrated that the peptoid-functionalized bicelle did not significantly alter the bicelle morphology. Based on the insertion properties of amphipathic peptoids into the lipids, we have designed a 15-mer peptoid oligomer that has a side chain structure similar to SMA copolymer at the 2:1 styrene:maleic acid molar ratio. Unlike the SMA copolymers, the synthesized peptoids have a much more uniform and controllable length, which in turn is expected to improve the stability and alignment of the macrodiscs.

## MATERIALS AND METHODS

### Peptoid synthesis

The 15-mer peptoid was synthesized on a robotic synthesizer using the submonomer solid-phase method (14). The synthesis started with swelling of the Rink amide resin (200 mg, 0.122 mmol) with N,N-dimethylformamide (DMF), followed by Fmoc deprotection. Specifically, the resin was treated with 40% piperidine in DMF (3 mL) for 3 min, followed by draining of the solution and addition of 40% piperidine in DMF (1.7 mL). The resin was agitated for another 12 min, the solution was drained, and the resin was washed with DMF (5 3 mL). The first step of the submonomer cycle was then started by the addition of 0.6 M bromoacetic acid solution in DMF (3.2 mL) and N, N⁰-di-isopropylcarbondiimide in DMF (1:1 v/v, 0.7 mL). The resin was agitated for 25 min, the solution was drained, and the resin was subjected to another wash cycle with DMF (5 3 mL). The second step of the submonomer cycle was next performed with the addition of a 1.5 M solution of phenylethylamine or b-alanine tert-butyl ester in DMF (3.2 mL) for 1 h, before draining of the reagents and washing the resin with DMF (5 3 mL). The two-step submonomer cycle was repeated until completion of the 15-mer peptoid. After automated synthe-sis, and the peptoid was acetylated using a 10% acetic acid solution in DMF (2 mL) for 30 min. The solution was drained, and the resin was washed with DMF (5 2 mL) and $CH_2Cl_2$ (5 2 mL). The peptoid was then cleaved from the resin, with removal of the side chain protecting groups using a solution of 95% trifluoroacetic acid and 5% water for 3 h. Evaporation of the cleavage cocktail filtrate, followed by purification us-ing reverse-phase high-performance liquid chromatography, afforded the desired peptoid in 5% overall yield and 98% purity. The 15-mer peptoid synthesized with 2:1 phenyl:carboxyl monomer ratio is shown in Fig. 1, which allows for their spontaneous incorporation into DMPC lipid for the formation of magnetically alignable peptoid-based macrodiscs.

### Preparation of protein-containing peptoid macrodiscs

The lipids used were purchased from Avanti Polar Lipids (Alabaster, AL, USA). The peptoid solution was prepared by dissolving the dry compound in 20 mM HEPES and 0.02% $NaN_3$ to 10 mg/mL final concentration and adjusting the pH to 8.0. Blank peptoid-DMPC macrodiscs were prepared with 1:22 to 1:27 peptoid:lipid molar ratios at 15% (w/v) lipid concentration in a 200 mL sample (20 mM HEPES, 0.02% $NaN_3$ [pH 8.0]). The Pf1 sample in peptoid macrodiscs was made by mixing 3 mg of Pf1 coat protein (expressed as described elsewhere (33)). The coat protein isolated from the phage through precipitation by adding TFE (50%) and trifluoroacetic acid (0.1%), followed by lyophilization and several washing steps. Lyophilized protein was dissolved in TFE, added to the lyophilized DMPC lipids thin film, vortexed, and dried to form a thin film under the nitrogen gas. The protein/lipid mixture was lyophilized overnight and rehydrated with 0.7 mL of 20 mM HEPES and 0.02% $NaN_3$ (pH 8.0) buffer followed by 3 steps of freeze-thaw cycle, then the peptoid was added in 3 aliquots totaling 0.3 mL. The samples were subjected to several temperature cycles (ice/$N_{2(liq.)}$/40C) after each aliquot addition, and solution was then concentrated down to 200 mL using 10,000 MWCO centrifuge filters. The concentrated sample was subjected to 5 more temperature cycles.

### Preparation of 14-mer peptide macrodiscs, SMA macrodiscs, and bicelles

A 14-mer belt peptide (Ac-DYLKAFYDKLKEAF-NH2) was purchased from Peptide 2.0 (Chantilly, VA, USA). A protocol for making macrodiscs using 14-mer has been previously described (10). Briefly, the peptide was solubilized in 20 mM HEPES (pH 8.0) at a final concentration of 35 mg/mL. The protein/lipid film, prepared as described above, was lyophilized overnight, rehydrated with the belt peptide solution, and subjected to several temperature cycles (ice, vortex, 40C, vortex, etc.). The final 200 mL NMR sample had a 10% (w/v) DMPC lipid (20 mg), a 5:1 (w/w) or 13.3:1 molar ratio of DMPC to 14-mer belt peptide (4 mg), and about 2 mg of Pf1 coat protein. To prepare the sample of SMA macrodiscs, 46 mL of the 6.7 mM solution (re-calibrated by drying, weighing, and rehydrating of the commercial stock solution) of 7.5 kDa SMA polymer (Cray Valley, Ex-ton, PA, USA; 2:1 styrene:maleic acid ratio) were gradually added to form a 200 mL solution of 10% w/v DMPC liposomes containing ca. 2 mg of Pf1 in a buffer (20 mM HEPES, 0.02% NaN3 [pH 8.0]), followed by multiple freeze-thaw cycles (ice/$N_{2(liq.)}$/40C) to form macrodiscs. The final molar ratio of lipids:SMA was 50:1. The Pf1-containing bicelle sample was prepared using well-established protocols (34,35).

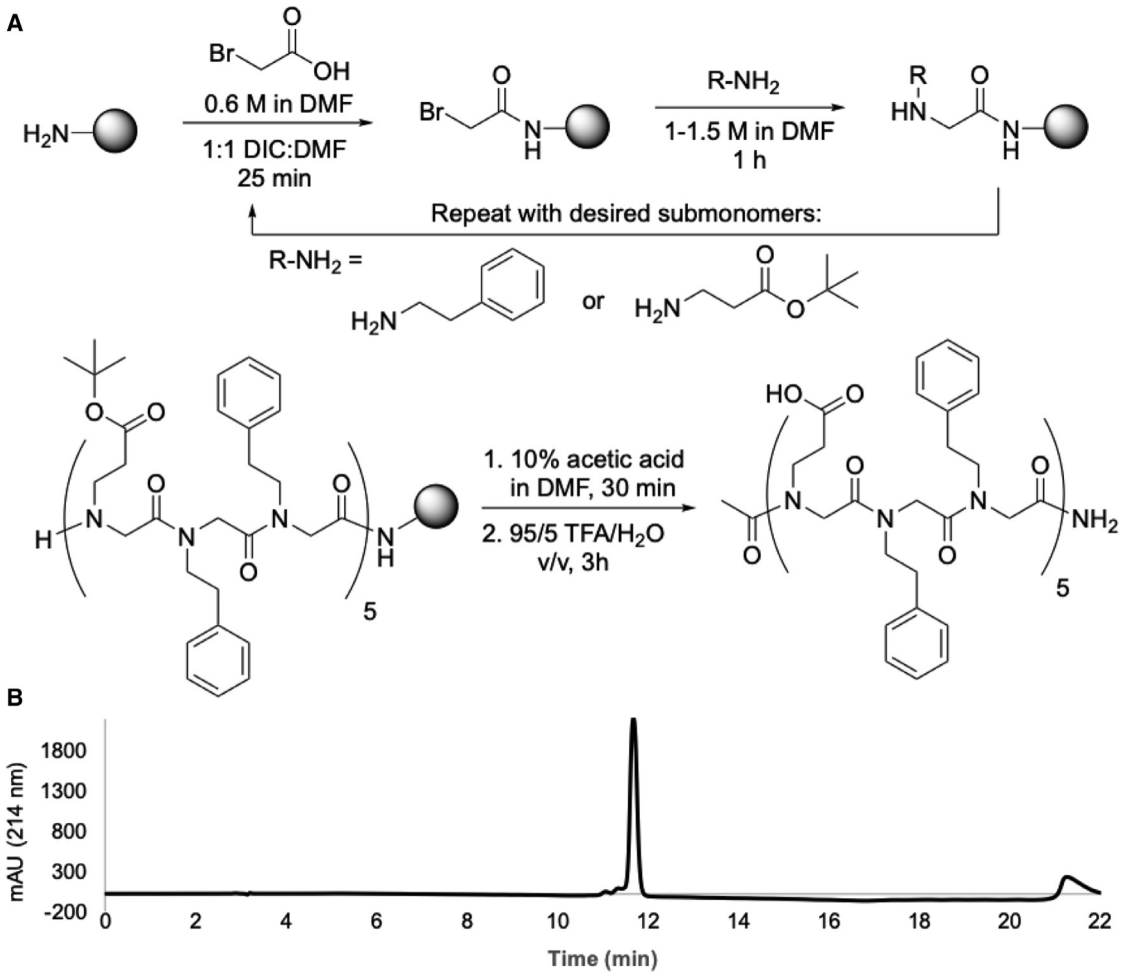


FIGURE 1 (A) Schematic for synthesis of 15-mer peptoid with the chemical formula $C_{127}H_{150}N_{16}O_{26}$ and a total molecular weight of 2.3 kDa. (B) Liquid chromatography with tandem mass spectrometry spectrum of the synthesized peptoid demonstrating sample purity at 214 nm.

## Dynamic light scattering (DLS)

The peptoid-macrodisc DLS measurements were performed on a Zetasizer nanoseries instrument (Malvern Instruments, Malvern, UK). The samples were diluted 40-fold from the NMR concentration using deionized water passed through the 0.2 mm membrane filter, and experiments were measured in a disposable 40 mL micro cuvette at 25C and 40C. All DLS measurements were collected for 30 s using 10 scans.

## NMR spectroscopy

All NMR experiments were acquired on an Avance II spectrometer (Bruker Biospin, Billerica, MA, USA) operating at a $^{1}$H NMR frequency of 500 MHz, and data were acquired using the Topspin 2.0 software. The NMR samples were sealed in a 5 mm glass tube and placed either in a static triple resonance $^{1}$H/$^{15}$N/$^{31}$P Bruker 5 mm E-free probe or a custom-made triple-resonance probe manufactured by BlackFox (Tallahassee, FL, USA). The $^{31}$P NMR spectra were acquired using a 20 ms 90 pulse with $^{1}$H decoupling. The $^{15}$N spectra were acquired at B1 rf field of either 60 (in the case of the BlackFox probe) or 48 kHz (in the case of the Bruker probe). Two-dimensional (2D) separated local field (SLF) spectra for both the bicelle and peptoid samples were acquired using the recently developed ROULETTE 2.0 pulse sequence (36) using the BlackFox probe (with a 20 ms acquisition in the direct dimension), whereas the previously published 14-mer peptide macrodisc spectrum (37) was acquired with SAMPI4 pulse sequence (38) and the commercial Bruker probe (also with the 20 ms acquisition in the direct dimension). The NMR data were processed and analyzed using NMRPipe (39). No apodization has been applied in the $^{15}$N chemical shift anisotropy (CSA) dimension for the data analysis.

## Transmission electorn microscopy (TEM) measurements

All TEM images were acquired on a Bio-TEM HT7800 120kV transmission electron microscope (Hitachi, Tokyo, Japan). The carbon-coated copper TEM grids were prepared by depositing 3 mL of diluted peptoid macrodics solution with a final lipid concentration of 40 mM on a grid. The grids were carefully dried with a filter paper and stained with 2% uranyl acetate solution, washed with the deionized water, and placed on the racks to dry overnight prior to the image acquisition.

# RESULTS

The size distribution of the peptoid-DMPC discs ultimately determines the quality of solid-state NMR spectra. One way to estimate the size distribution of the peptoid macrodisc

particle as it diffuses in the sample solution is by DLS. The nature of DLS requires fairly dilute solutions in order to minimize the multiple scattering through the sample, so the samples were diluted 40-fold prior to the measurements. The polydispersity index, which is a representation of the variance of size distribution, exhibits a value of 0.155 (cf. Fig. 2), which may be partially due to different scattering angles from the anisotropic discoidal species. The $Z_{avg}$ diameter is the most direct way to measure the particle, and it is derived from single exponential fit of the light scattering autocorrelation function assuming single particle size, but it does not provide for a size distribution. A distribution by volume, on the other hand, is obtained from scattering intensity distribution with the consideration that particles of different sizes scatter different intensities of light under the assumption that particles are homogenous and spherical. The results of the measurements demonstrated on Fig. 2 show the presence of the macrodiscs with the Z average diameter of 40 nm. It should be emphasized that DLS data analysis is based on the assumption of spherical particle shapes, while in fact we are dealing with discoidal species, which may skew the distributions toward smaller sizes.

To further investigate the morphology of the peptoid-based macrodiscs, we turned to the negative-stain TEM. On the micrographs shown in Fig. 2, the discs with approximate diameters of 40 nm are observed either as clusters (B) or individually (C). Rare occurrences of the discs that are positioned either perpendicularly or at an angle with respect to the surface of the grid may be due to the extensive wash of the grids prior to image acquisition. Additional TEM images showing discs lying on their side are provided in the supporting material. Importantly, the size of the species observed on the TEM images is in agreement with the above $Z_{avg}$ diameter value of 42 nm.

Solid-state NMR experiments were subsequently carried out after confirming that the lipo-peptoid complexes possess a discoidal morphology and are large enough for a spontaneous alignment in the presence of an external magnetic field. Both $^{31}$P NMR and $^{15}$N NMR spectra are in agreement with the results of the DLS and TEM measurements, proving an effective and uniform sample alignment (cf. Fig. 3).

The $^{31}$P NMR spectrum of a sample containing 3.2 mg Pf1 coat protein reconstituted in peptoid-based macrodisc (Fig. 3 A) shows a single anisotropic chemical shift at ca. 13.5 ppm

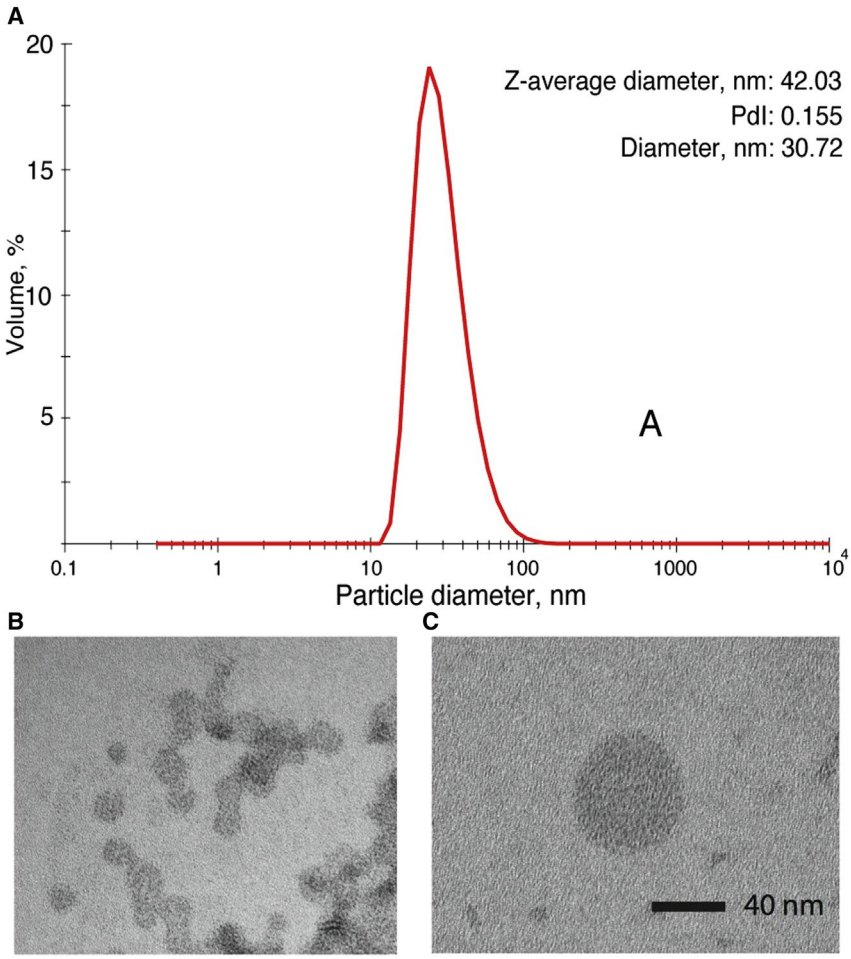


FIGURE 2 (A) Dynamic light scattering particle-size distribution by volume for a diluted peptoid macrodisc sample measured at 25C. Polydispersity index and $Z_{avg}$ diameter are shown as insets in the top right corner. (B) Transmission electron microscopy images of the peptoid-based macrodiscs loaded with Pf1 coat protein demonstrating the presence of clusters of discs with an average diameter of 40 nm. (C) An enlarged image of an individual disc with the black bar as a scale. To see this figure in color, go online.

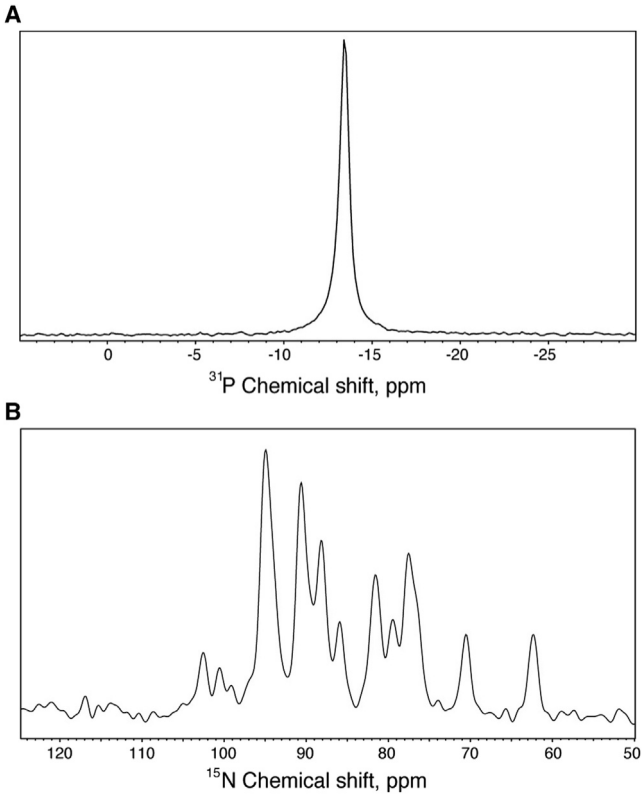


FIGURE 3 (A) $^{31}$P chemical shift NMR spectrum of the sample of Pf1 coat protein reconstituted in peptoid-belt macrodiscs, at a sample temperature of 37C and 23:1 lipid:peptoid molar ratio. (B) One-dimensional $^{15}$N NMR spectrum of Pf1 coat protein reconstituted in peptoid-based macrodiscs measured at 37C.

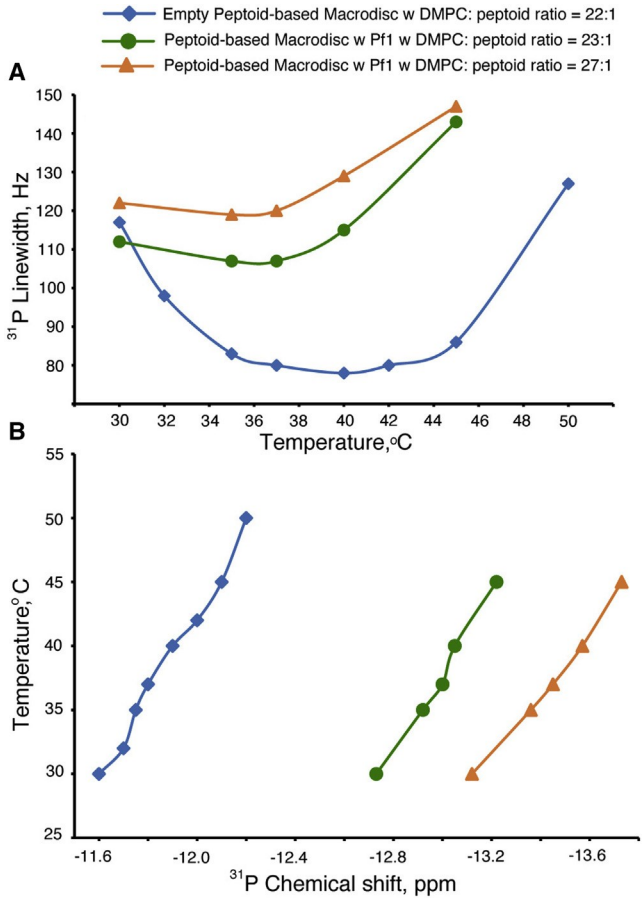


FIGURE 4 The effect of temperature on the $^{31}$P NMR linewidth (A) and resonance position (B) at various lipid:peptoid ratios and presence of the incorporated membrane protein as indicated. To see this figure in color, go online.

having a 120 Hz linewidth, which is to be compared with the typical 150–200 Hz observed in bicelles. Fig. 3 B shows a one-dimensional $^{15}$N chemical shift spectrum of uniformly labeled Pf1 coat protein in the peptoid-based macrodiscs. The spectrum shows well-resolved $^{15}$N resonances arising from the residues corresponding to the aligned transmembrane helix region (60–110 ppm). It should be noted that a low degree of polydispersity of the sample, as observed by DLS and TEM, ultimately determines the high quality of the spectra and that there are no "isotropic" or unaligned peaks in the $^{31}$P NMR spectrum. The optimal temperature of alignment was found to be 37C based on the $^{31}$P NMR measurements, as summarized in Fig. 4.

Fig. 4 shows the effect of temperature on the magnetic alignment of the macrodiscs. The $^{31}$P NMR resonance shifts to the right (toward higher negative ppm values), while the $^{31}$P linewidth passes through a minimum. This trend for the resonance shift persists until a certain upper limit (45C–50C), where the high temperature starts to negatively affect the overall stability of the complex. Still, the peptoid-based discs remain aligned over a wide temperature range, from ca. 30C to at least 45C. Additional 1D $^{31}$P and 2D $^{15}$N NMR spectra measured at as low as 25C are presented in the supporting material. While the order parameter has further increased to ca. 0.9 at this temperature, static orientational disorder becomes more pronounced, which, in turn, negatively affects resolution. Furthermore, as the size of the macrodisc increases (i.e., at higher lipid:peptoid ratios), a greater degree of alignment is observed (i.e., higher anisotropic ppm values). However, due to its larger size, the disc likely experiences slower motions, and hence an increase in the NMR linewidths is observed due to less efficient motional narrowing. Note that when loaded with the Pf1 coat protein, the optimal $^{31}$P NMR linewidth slightly increases from ca. 78 to ca. 107 Hz compared with the pure macrodiscs.

The advantages of peptoid-based macrodiscs compared with other membrane-mimicking systems used for OS NMR become even more apparent for the case of 2D SLF NMR spectra. Fig. 5 A shows an overlay of SLF spectra of Pf1 coat protein in the various alignment mimics (i.e., bicelles, peptide macrodiscs, and peptoid-based discs). NMR data for membrane mimetics based on styrene/maleic acid copolymer belts are given in the supporting material. Suboptimal resolution obtained in $^{15}$N NMR spectra of Pf1 coat protein in the latter case is possibly due to a lower degree of

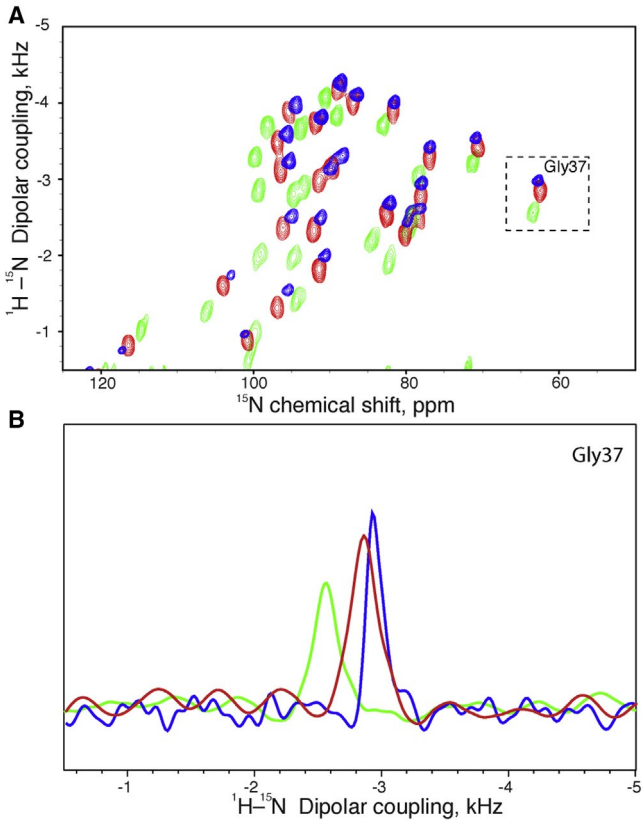


FIGURE 5 (A) Two-dimensional NMR spectra of Pf1 reconstituted in different membrane mimics: the "traditional" q ¼ 3.2 DMPC/DHPC bicelles (green), 14-mer belt peptide-DMPC macrodiscs (red), and 15-mer peptoid-DMPC macrodiscs (blue). (B) Slices through the dipolar dimension for peak G37 from the spectrum of panel A.

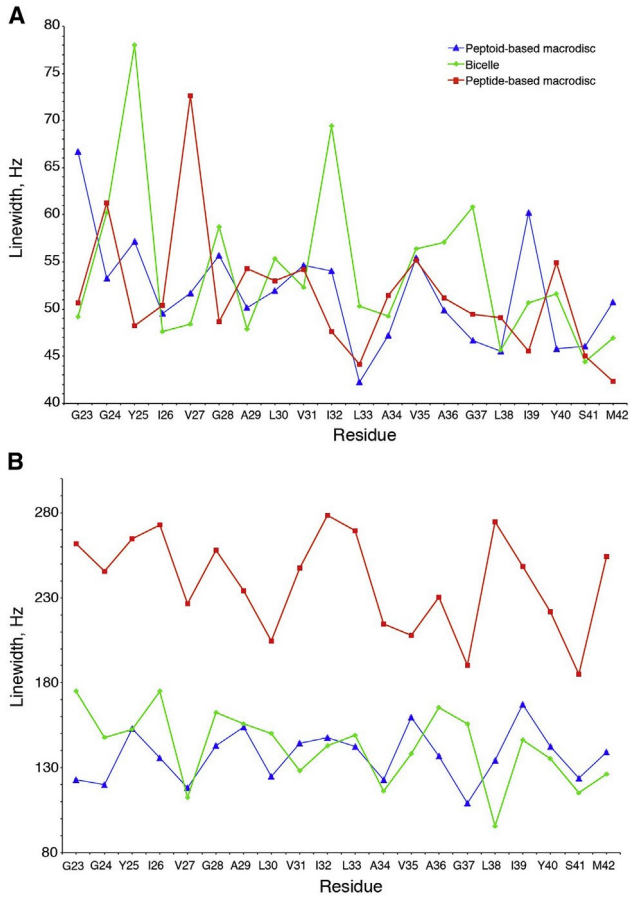


FIGURE 6 (A and B) Chemical shift anisotropy (A) and dipolar (B) line widths measured at half height for each assigned TM residue in the $^{15}$N chemical shift anisotropy and $^{1}$H-$^{15}$N dipolar dimensions from two-dimensional NMR spectra: q ¼ 3.2 DMPC/DHPC bicelles (green), belt peptide-DMPC macrodisc (red), and in 15-mer peptoid-DMPC macrodiscs (blue). The connecting lines are shown as a visual guide. More uniform chemical shift anisotropy linewidths are obtained in the case of peptoid-based macrodiscs, indicating a more homogenous rotational motional averaging.

magnetic alignment of SMA macrodiscs at the field strength used in this work (11.7 T) versus that used in (12) (21.1 T). A direct comparison of 2D NMR spectra in Fig. 5 A shows a measurable increase in the order parameter for the peptoid macrodiscs, as evidenced by an increased range for the dipolar coupling when compared with DMPC/DHPC bicelles and the previously published 14-mer belt peptide macrodiscs (37).

The increase in the dipolar coupling range (from ca. 4.0 to 4.3 kHz) for the maximum coupling indicates a higher degree of magnetic alignment in the case of peptoid-based discs, quantitatively corresponding to an increase in the order parameter from 0.8 to 0.86, compared with bicelles. Note that there are concomitant systematic displacements in the chemical shifts in the direction away from the isotropic value (120 ppm), thus also indicating an increased degree of alignment. Fig. 5 B shows slices through the indirect dimension for the resolved peaks for residue G37 comparing the dipolar shapes linewidths for the three lipid mimetics.

Fig. 6 summarizes direct comparisons of the spectral linewidths in the CSA and dipolar NMR dimensions measured for each transmembrane peak in the assigned SLF spectra of Pf1 coat protein. Note that while all three profiles approximately follow a 3.6-periodicity characteristic of OS NMR observables for an a-helix, the CSA linewidths measured for peptoid macrodics in Fig. 6 A are more uniform (blue lines). This would indicate a more homogeneous motional narrowing of the dipolar NMR lines due to fast uniaxial rotational diffusion, which is essential for obtaining good resolution at the perpendicular membrane alignment relative to the main magnetic field (40). Sharper dipolar linewidths are observed for the peptoid sample and bicelles compared with the belt-peptide lipodiscs (cf. Fig. 6 B). However, the narrower dipolar linewidths measured for peptoid-based macrodiscs and bicelles versus lipodiscs are likely due to the higher efficiency of ROULETTE versus SAMPI4 used to evolve the vertical (indirect) NMR dimension. It should also be noted that SMA- and peptide-based macrodiscs typically incorporate ca. 2 mg of the protein in a 180 mL sample, whereas the loading by the Pf1 coat protein in the case of peptoid-based macrodiscs is increased here to 3.2 mg for the same sample volume.

## CONCLUSIONS

Similarly to bicelles and macrodiscs stabilized with either belt peptides or SMA polymers, peptoid-based macrodiscs have been shown here to act as a self-assembled, magnetically orientable membrane mimetics for OS NMR studies of MPs. The peptoid-based macrodiscs are able to incorporate and align MPs, resulting in well-resolved resonances as demonstrated by systematic NMR studies performed with the membrane-reconstituted Pf1 coat protein. Both $^{31}$P and $^{15}$N NMR experiments have demonstrated that the peptoid macrodisc yields high uniformity of the magnetic alignment and increased order parameter in comparison with bicelles and lipoprotein-based macrodiscs.

While the formation of a stable membrane mimic based on 15-mer peptoids has been demonstrated here for the first time, the controllable peptoid synthesis affords for further tuning and control of the disc diameter, size distribution, and protein loading factors. Moreover, the peptoid-based mimetics developed in the present work yield a sufficiently uniform size distribution given the relatively simple sample preparation protocol, which does not require additional size-exclusion and purification steps. The DLS data show that the peptoid-based macrodiscs with a relatively narrow distribution of ca. 40–50 nm particles are consistent with the observed narrow $^{31}$P signal arising from uniformly aligned species. A noticeable improvement in the ordering and, thus, the spectral range and uniform resolution was observed in the 2D NMR spectra of Pf1 coat protein reconstituted in magnetically aligned peptoid-based macrodiscs versus DMPC/DHPC bicelles and belt peptide-DMPC macrodiscs. While the linewidths in the dipolar dimension for the peptoid-based discs and bicelles have been found to be similar on average, the former are completely detergent free and possess a tunable discoidal morphology. On-going and future research efforts are aimed at studying mixtures of polyunsaturated lipids and cholesterol embedded in peptoid-based macrodiscs with the purpose of investigating lipid-protein interactions, membrane fluidity, and lipid rafts. The presented magnetically alignable membrane mimetic is potentially applicable to solid-state NMR studies of more complex, multi-span MPs.

## SUPPORTING MATERIAL

Supporting material can be found online at https://doi.org/10.1016/j.bpj.2022.07.024.

## AUTHOR CONTRIBUTIONS

A.R.G., R.J.A.E., and E.O.A. have prepared NMR samples and performed the NMR experiments and analyses of the obtained results. A.R.G., R.J.A.E., and A.A.N. wrote the manuscript. C.M.D. and Q.A.E.G. performed the synthesis of the peptoids and their characterization. C.P. supervised the synthetic part of the project, and A.A.N. supervised the NMR part of the project. All authors discussed the results and contributed to the final manuscript.

## ACKNOWLEDGMENTS

This material is based upon work supported by the National Science Foundation under grant no. MCB 1818240 and by the US Army Research Office under contract number W911NF1810363. TEM was performed at the Analytical Instrumentation Facility (AIF) at North Carolina State University, which is supported by the state of North Carolina and the National Science Foundation (award number ECCS-2025064). The AIF is a member of the North Carolina Research Triangle Nanotechnology Network (RTNN), a site in the National Nanotechnology Coordinated Infrastructure (NNCI). We thank Prof. Francesca Marassi (The Sanford-Burnham-Prebys Medical Discovery Institute) for fruitful discussions.

## DECLARATION OF INTERESTS

The authors declare no competing interests.

## REFERENCES

1. Sanders, C. R., and J. H. Prestegard. 1990. Magnetically orientable phospholipid bilayers containing small amounts of a bile salt analogue, CHAPSO. Biophys. J. 58:447–460.
2. Sanders, C. R., and J. P. Schwonek. 1992. Characterization of magnetically orientable bilayers in mixtures of DHPC and DMPC by solid state NMR. Biochemistry. 31:8898–8905.
3. Vold, R. R., and R. Prosser. 1996. Magnetically oriented phospholipid bilayered micelles for structural studies of polypeptides. Does the ideal bicelle exist? J. Magn. Reson. B. 113:267–271.
4. Prosser, R. S., J. S. Hwang, and R. R. Vold. 1998. Magnetically aligned phospholipid bilayers with positive ordering: a new model membrane system. Biophys. J. 74:2405–2418.
5. Glover, K. J., J. A. Whiles, . , R. R. Vold. 2001. Structural evaluation of phospholipid bicelles for solution-state studies of membrane-associated biomolecules. Biophys. J. 81:2163–2171.
6. Verardi, R., N. J. Traaseth, . , A. Scaloni. 2011. Probing membrane topology of the antimicrobial peptide distinctin by solid-state NMR spectroscopy in zwitterionic and charged lipid bilayers. Biochim. Biophys. Acta. 1808:34–40.
7. Dürr, U. H. N., M. Gildenberg, and A. Ramamoorthy. 2012. The magic of bicelles lights up membrane protein structure. Chem. Rev. 112:6054–6074.
8. Gayen, A., J. R. Banigan, and N. J. Traaseth. 2013. Ligand-induced conformational changes of the multidrug resistance transporter EmrE probed by oriented solid-state NMR spectroscopy. Angew. Chem. Int. Ed. Engl. 52:10321–10324.
9. Scholz, F., E. Boroske, and W. Helfrich. 1984. Magnetic-anisotropy of lecithin membranes - a new anisotropy susceptometer. Biophys. J. 45:589–592.
10. Park, S. H., S. Berkamp, . , S. J. Opella. 2011. Nanodiscs versus macrodiscs for NMR of membrane proteins. Biochemistry. 50:8983–8985.
11. Ravula, T., S. K. Ramadugu, . , A. Ramamoorthy. 2017. Bioinspired, size-tunable self-assembly of polymer-lipid bilayer nanodiscs. Angew. Chem. Int. Ed. Engl. 56:11466–11470.
12. Radoicic, J., S. H. Park, and S. J. Opella. 2018. Macrodiscs comprising SMALPs for oriented sample solid-state NMR spectroscopy of membrane proteins. Biophys. J. 115:22–25.
13. Park, S. H., J. Wu, . , S. J. Opella. 2020. Membrane proteins in magnetically aligned phospholipid polymer discs for solid-state NMR spectroscopy. Biochim. Biophys. Acta Biomembr. 1862:183333.

14. Zuckermann, R. N., J. M. Kerr, . , W. H. Moos. 1992. Efficient method for the preparation of peptoids oligo(N-substituted glycines) by submonomer solid-phase synthesis. J. Am. Chem. Soc. 114:10646–10647.
15. Zuckermann, R. N., and T. Kodadek. 2009. Peptoids as potential therapeutics. Curr. Opin. Mol. Ther. 11:299–307.
16. Sun, J., and R. N. Zuckermann. 2013. Peptoid polymers: a highly designable bioinspired material. ACS Nano. 7:4715–4732.
17. Fowler, S. A., and H. E. Blackwell. 2009. Structure-function relationships in peptoids: recent advances toward deciphering the structural requirements for biological function. Org. Biomol. Chem. 7:1508–1524.
18. Mojsoska, B., R. N. Zuckermann, and H. Jenssen. 2015. Structure-activity relationship study of novel peptoids that mimic the structure of antimicrobial peptides. Antimicrob. Agents Chemother. 59:4112–4120.
19. Molchanova, N., P. R. Hansen, and H. Franzyk. 2017. Advances in development of antimicrobial peptidomimetics as potential drugs. Molecules. 22:E1430.
20. Armand, P., K. Kirshenbaum, . , E. K. Bradley. 1998. NMR determination of the major solution conformation of a peptoid pentamer with chiral side chains. Proc. Natl. Acad. Sci. USA. 95:4309–4314.
21. Wu, C. W., T. J. Sanborn, ., A. E. Barron. 2001. Peptoid oligomers with alpha-chiral, aromatic side chains: sequence requirements for the formation of stable peptoid helices. J. Am. Chem. Soc. 123:6778–6784.
22. Wu, C. W., T. J. Sanborn, . , A. E. Barron. 2001. Peptoid oligomers with alpha-chiral, aromatic side chains: effects of chain length on secondary structure. J. Am. Chem. Soc. 123:2958–2963.
23. Wu, C. W., K. Kirshenbaum, . , A. E. Barron. 2003. Structural and spectroscopic studies of peptoid oligomers with alpha-chiral aliphatic side chains. J. Am. Chem. Soc. 125:13525–13530.
24. Stringer, J. R., J. A. Crapster, . , H. E. Blackwell. 2011. Extraordinarily robust polyproline type I peptoid helices generated via the incorporation of alpha-chiral aromatic N-1-Naphthylethyl side chains. J. Am. Chem. Soc. 133:15559–15567.
25. Armand, P., K. Kirshenbaum, . , F. E. Cohen. 1997. Chiral N-substituted glycines can form stable helical conformations. Fold. Des. 2:369–375.
26. Gorske, B. C., J. R. Stringer, . , H. E. Blackwell. 2009. New strategies for the design of folded peptoids revealed by a survey of noncovalent interactions in model systems. J. Am. Chem. Soc. 131:16555–16567.
27. Zhang, Y., S. Xuan, . , V. T. John. 2017. Amphiphilic polypeptoids serve as the connective glue to transform liposomes into multilamellar structures with closely spaced bilayers. Langmuir. 33:2780–2789.
28. Zhang, Y., Z. Heidari, . , V. John. 2019. Amphiphilic polypeptoids rupture vesicle bilayers to form peptoid-lipid fragments effective in enhancing hydrophobic drug delivery. Langmuir. 35:15335–15343.
29. Jing, X., M. R. Kasimova, . , H. M. Nielsen. 2012. Interaction of peptidomimetics with bilayer membranes: biophysical characterization and cellular uptake. Langmuir. 28:5167–5175.
30. Andreev, K., M. W. Martynowycz, . , D. Gidalevitz. 2018. Hydrophobic interactions modulate antimicrobial peptoid selectivity towards anionic lipid membranes. Biochim. Biophys. Acta Biomembr. 1860:1414–1423.
31. Landry, M. R., J. L. Rangel, . , G. Y. Stokes. 2019. Length and charge of water-soluble peptoids impact binding to phospholipid membranes. J. Phys. Chem. B. 123:5822–5831.
32. Najafi, H., and S. L. Servoss. 2018. Altering the edge chemistry of bicelles with peptoids. Chem. Phys. Lipids. 217:43–50.
33. Thiriot, D. S., A. A. Nevzorov, . , S. J. Opella. 2004. Structure of the coat protein in Pfl bacteriophage determined by solid-state NMR spectroscopy. J. Mol. Biol. 341:869–879.
34. De Angelis, A. A., A. A. Nevzorov, . , S. J. Opella. 2004. High-resolution NMR spectroscopy of membrane proteins in "unflipped" bicelles. J. Am. Chem. Soc. 126:15340–15341.
35. Park, S. H., F. M. Marassi, ., S. J. Opella. 2010. Structure and dynamics of the membrane-bound form of Pf1 coat protein: implications of structural rearrangement for virus assembly. Biophys. J. 99:1465–1474.
36. Lapin, J., and A. A. Nevzorov. 2020. Computer-generated pulse sequences for 1H-15N and 1Ha-13Ca Separated local-field experiments. J. Magn. Reson. 317:106794.
37. Tesch, D. M., Z. Pourmoazzen, . , A. A. Nevzorov. 2018. Uniaxial diffusional narrowing of NMR lineshapes for membrane proteins reconstituted in magnetically aligned bicelles and macrodiscs. Appl. Magn. Reson. 49:1335–1353.
38. Nevzorov, A. A., and S. J. Opella. 2007. Selective averaging for high-resolution solid-state NMR spectroscopy of aligned samples. J. Magn. Reson. 185:59–70.
39. Delaglio, F., S. Grzesiek, . , A. Bax. 1995. NMRPipe: a multidimensional spectral processing system based on UNIX pipes. J. Biomol. NMR. 6:277–293.
40. Nevzorov, A. A. 2011. Orientational and motional narrowing of solid-state NMR lineshapes of uniaxially aligned membrane proteins. J. Phys. Chem. B. 115:15406–15414.